We are IntechOpen,
the world's leading publisher of
Open Access books
Built by scientists, for scientists

4,800
Open access books available

122,000
International authors and editors

135M
Downloads

Our authors are among the

154
Countries delivered to

TOP 1%
most cited scientists

12.2%
Contributors from top 500 universities

CLARIVATE ANALYTICS
BOOK CITATION INDEX
INDEXED

WEB OF SCIENCE™

Selection of our books indexed in the Book Citation Index
in Web of Science™ Core Collection (BKCI)

Interested in publishing with us?
Contact book.department@intechopen.com

Numbers displayed above are based on latest data collected.
For more information visit www.intechopen.com

Ultrastructure and Topochemistry of Plant Cell Wall by Transmission Electron Microscopy

Xia Zhou, Dayong Ding, Jing Ma, Zhe Ji,
Xun Zhang and Feng Xu

Additional information is available at the end of the chapter

Abstract

Plant cell walls are typically described as complex macromolecular composites consisting of an ordered array of cellulose microfibrils embedded in a matrix of non-cellulosic polysaccharides and lignin. Generally, the plant cell wall can be divided into three major layers: middle lamella, primary cell wall, and secondary cell wall. Investigation of plant cell walls is complicated by the heterogeneous and complex hierarchical structure, as well as variable chemical composition between different sub-layers. Thus, a complete understanding of the ultrastructure of plant cell walls is necessary. Transmission electron microscopy (TEM) has proven to be a powerful tool in elucidating fine details of plant cell walls at nanoscale. The present chapter describes the layering structure and topochemistry of plant cell wall revealed by TEM.

Keywords: Plant cell wall, Transmission electron microscopy, Ultrastructure, Topo-chemistry

1. Introduction

Determining the ultrastructural organization of plant cell walls represents one of the most challenging problems in plant biology. Although considerable progress has been made in understanding the basic organization and functions of plant cell wall components, due to the highly complex and dynamic nature of the plant cell wall, the variation in cell wall architecture of wood and gramineous species remains poorly understood. These structural features are

associated with cell growth and morphogenesis, which are also crucial in determining the mechanical properties of plant cell walls [1, 2]. Given that one of the critical processing steps in biomass conversion involves systematic deconstruction of cell walls, this structural information is also pivotal for developing novel approaches to convert biomass into liquid biofuels. Therefore, a comprehensive investigation of the architecture of the plant cell wall will not only help us to understand the assembly and biosynthesis of the plant cell wall, but will also contribute to improving the efficiency of biomass deconstruction [3].

The plant cell wall is a layered construction composed mainly of stiff crystalline cellulose microfibrils (Mfs) embedded in an amorphous matrix of non-crystalline cellulose, hemicelluloses and pectin, as well as various aromatic compounds and proteins [4]. Besides the varieties of chemical constituents, the ultrastructural organization of plant cell wall varies between species and cell types. Generally, the plant cell wall consists of three major layers: (i) the middle lamella (Ml), (ii) the primary wall (Pw), and (iii) the secondary wall (Sw). Due to the highest thickness, Sw accounts for the largest proportion of the plant cell wall. Sw in higher plants consists mainly of cellulose, lignin, and xylan and is the major component of biomass in many species. In hardwood fibers and softwood tracheids, the Sw is normally further differentiated into an outer layer (S1), a middle layer (S2), and an inner layer (S3), with the S2 having the largest thickness [5, 6]. By comparison, in gramineous species the lamellation of the Sw in fiber is generally described as alternating broad and narrow layers [7].

In the twentieth century, microscopic approaches began to offer high-resolution images to enhance our understanding of cell wall organization. Over the past few decades, atomic force microscopy (AFM) has been successfully applied to high-resolution architecture, assembly, and structure dynamic studies of a wide range of biological systems, which has enabled researchers to visualize the ultrastructure of the plant cell wall [8, 9]. More recently, confocal Raman microspectroscopy (CRM) has now also been successfully applied to acquire information on the preferential orientation of plant polymer functional groups and components distribution in situ [10, 11]. However, although these approaches have been comprehensively used to obtain new information on cell wall architecture, until now the highly complex and dynamic nature of the plant cell wall at nanoscale has limited our ability to generate detailed structural models.

By comparison, due to the higher spatial resolution (<1nm) and specificity when combined with chemical staining and immunolabeling approaches, transmission electron microscopy (TEM) can provide ultrastructural and topochemical information simultaneously and has been used to investigate plant cell wall [12-14]. In this chapter, we mainly discuss the application of TEM in detecting cell wall layering structure and cell wall topochemistry (lignin distribution and hemicelluloses distribution).

2. Cell wall layering structure

To get any information using transmitted electrons in the TEM, specimens have to be thin. "Thin" is a relative term, in this context it means electron transparent. For a specimen to be

transparent to electrons, it must be thin enough to transmit sufficient electrons such that enough intensity falls on the screen, charge coupled device (CCD), or photographic plate to give an interpretable image in a reasonable time. Generally this requirement is a function of the electron energy and the average atomic number (Z) of the specimen. It is almost an axiom in TEM that thinner is better and specimens <100 nm should be used wherever possible. However, a too thin section would produce low-contrast TEM image, which hides the subtle structure. For plant cell wall, specimens are generally cut to a thickness of ~80 nm when they are silvery gold in color under ultramicrotome. In extreme cases such as doing high-resolution TEM (HRTEM) or electron spectrometry, specimen thicknesses <50 nm (even <10 nm) are essential.

2.1. Cell wall layering structure in hardwoods and softwoods

TEM examination showed that *Cornus alba* L. fiber cell wall was composed of three major layers: the middle lamella (ML) and the primary wall (P), and the secondary wall layer (S1, S2, and S3), a typical layering structure of fiber cell walls in other wood species [13, 15, 16]. The boundary between primary wall and middle lamella was not clearly distinguishable due to its high density and extreme thinness. Therefore, both the middle lamella (ML) and the contiguous primary wall (P) were referred here as compound middle lamella (CML) (Fig. 1a). The CML was electron dense, but the density was not uniform and this cell wall region had a mottled appearance containing dense and less dense or lucent regions. Inhomogeneity in lignin distribution in CML has also been reported in a few other TEM studies of hardwood species [17, 18]. The secondary wall was divided into an outer layer (F-S1), a middle layer (F-S2), and an inner layer (F-S3). The F-S1 layer in *Cornus alba* L. fiber was well-defined and can be readily distinguished from the adjoining F-S2 layer because of its higher electron density compared to F-S2 layer. The F-S1 layer was variable in width within and among cells (0.22–0.32 μm) (Table 1). The widest F-S2 layer accounted for the largest proportion of the fiber wall. Measurements of the width of fiber radial wall showed that the average thickness of the F-S2 layer was 2.67 μm. Fiber cell walls also contained an F-S3 layer that was very thin and not well developed.

Cell wall regions	Average thickness (range)	Standard deviation
F-S1	0.30 (0.22–0.32)	0.06
F-S2	2.67 (1.20–4.07)	0.14
V-S1	0.21 (0.18–0.32)	0.05
V-S2	0.62 (0.55–0.67)	0.17
AP-S3	0.73 (0.60–1.67)	0.19
RP-S1	0.61 (0.24–0.82)	0.14
RP-S2	0.80 (0.32–0.91)	0.27

Table 1. The average thickness of cell wall layers in *Cornus alba L.*

In addition to fiber cell wall, the ultrastructural variation in vessel, axial parenchyma, and ray parenchyma was also investigated. As shown in Fig. 1b, the vessel wall was divided into three layers (V-S1, V-S2, and V-S3) of variable electron density. The width of V-S1 ranged from 0.18 μm to 0.32 μm, approximately equal to that of F-S1, while the V-S2 was much thinner, with width from 0.55 μm to 0.67 μm. For the axial parenchyma (AP), the secondary wall was clearly resolved into an outer layer (AP-S1), a middle layer (AP-S2), and an inner layer (AP-S3) (Fig. 1c). Unlike the widest F-S2 layer accounting for the largest proportion of the secondary wall, in axial parenchyma the AP-S3 was the major proportion of secondary wall with the thickness ranging from 0.60 μm to 1.67 μm. In ray parenchyma (RP), the secondary wall consisted of two well-defined layers (outer layer, RP-S1, and inner layer, RP-S2), which did not fit conventional S1, S2, and S3 classification (Fig. 1d). Measurements taken on TEM micrograph evidenced that the average width of the RP-S1 was 0.61 μm, while the average thickness of the RP-S2 was 0.80 μm.
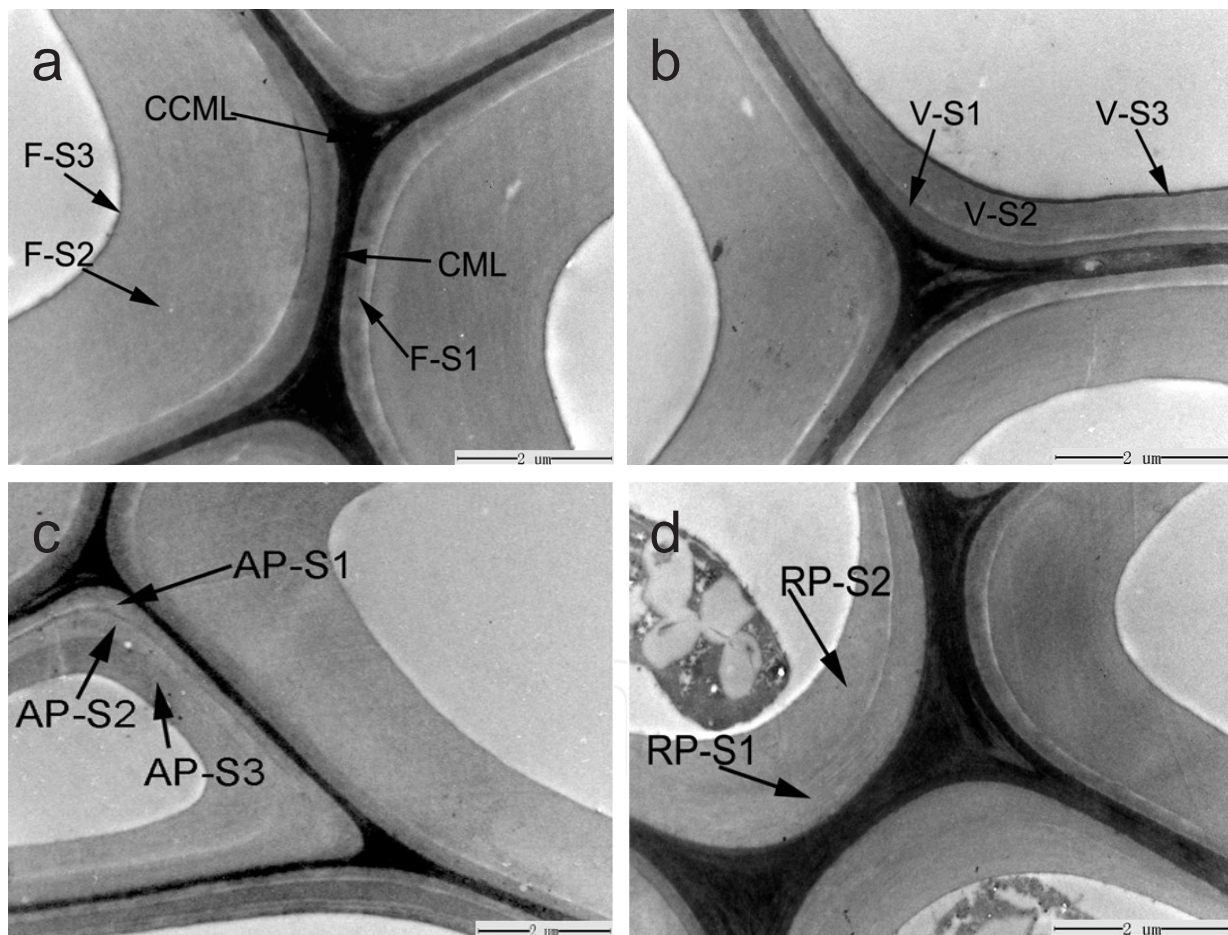

Figure 1. TEM micrographs of cross sections of *C. alba* L., taken at 80 kV. (a) CCML, cell corner middle lamella between adjoining fibers; CML, compound middle lamella between adjoining fibers; F-S1, outer secondary wall of fiber; F-S2, middle secondary wall of fiber; F-S3, inner secondary wall of fiber. (b) V-S1, outer secondary wall of vessel; V-S2, middle secondary wall of vessel; V-S3, inner secondary wall of vessel. (c) AP-S1, outer secondary wall of axial parenchyma; AP-S2, middle secondary wall of axial parenchyma; AP-S3, inner secondary wall of axial parenchyma. (d) RP-S1, outer secondary wall of ray parenchyma; RP-S2, inner secondary wall of ray parenchyma.

The ultrastructure of pit membrane (PM) among various wood elements (inter-fiber, fiber-vessel, fiber-axial parenchyma, and fiber-ray parenchyma) was also investigated. The thickness of PM varied considerably, with PM between fiber and ray parenchyma having a mean thickness of 500 nm, while PM between fiber and vessel had an average thickness of 220 nm. Thin PM with an average thickness of 230 nm was also found between parenchyma cells. PM varied also in their electron density, with inter-fiber PM (Fig. 2a) appearing distinctly denser than fiber-vessel (Fig. 2b) and fiber-parenchyma (axial and ray parenchyma) PM (Fig. 2c and 2d), which may reflect textural and/or compositional differences. The electron density variations originated from the deposition of lignin that is directly and linearly proportional to lignin concentration [13]. Thus, we can assume that the inter-fiber PMs have the highest lignin concentration, followed by fiber and parenchyma (axial and ray parenchyma) and fewest in the PM between fiber and vessel.
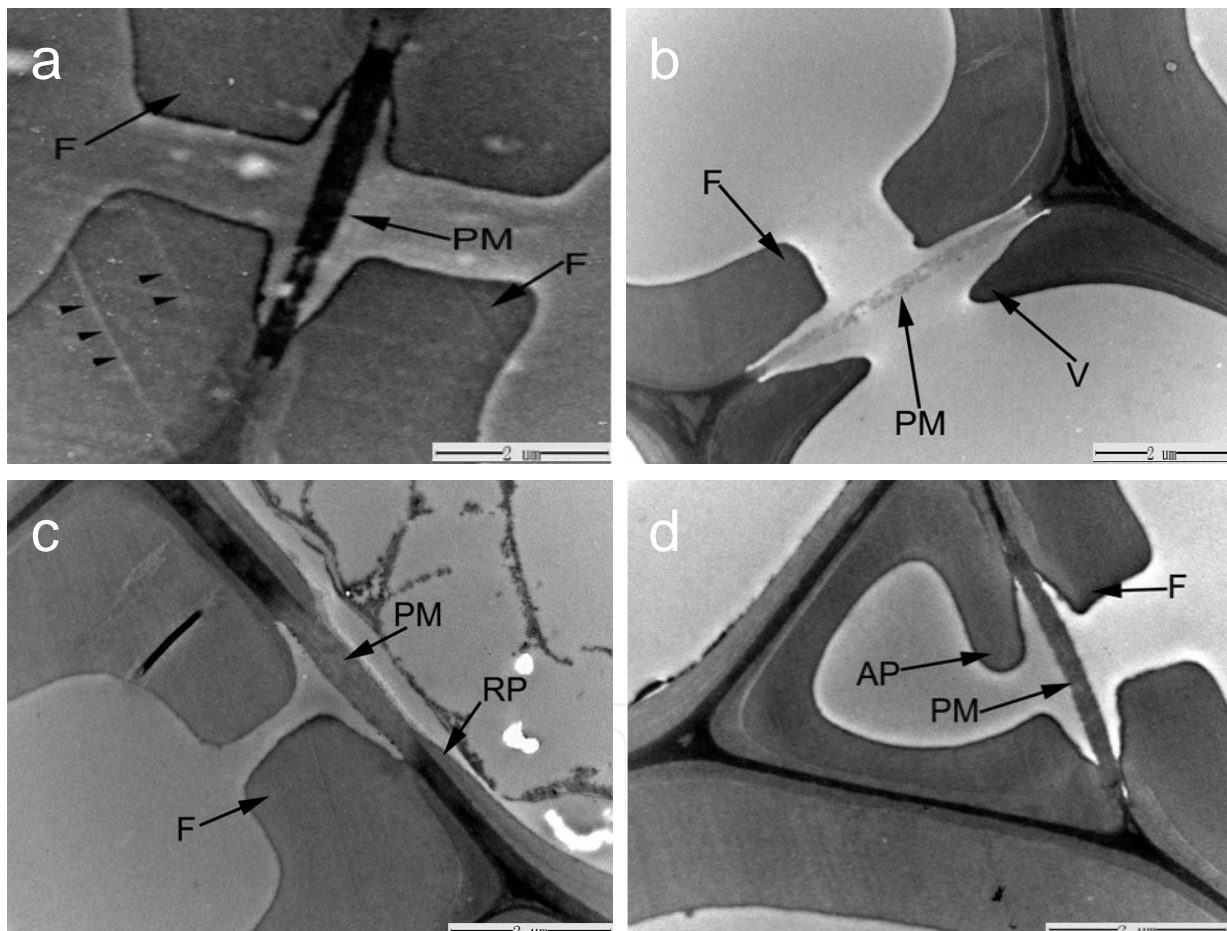

Figure 2. TEM micrographs of pit membrane among various cells in *C. alba* L., taken at 80 kV. (a) Pit membrane between fibers, (arrowheads: knife mark). (b) Pit membrane between fiber and vessel. (c) Pit membrane between fiber and ray parenchyma. (d) Pit membrane between fiber and axial parenchyma. F, fiber; V, vessel; RP, ray parenchyma; AP, axial parenchyma; PM, pit membrane.

Compared to hardwood, the cell type of softwood is uniform, mainly containing tracheids. In normal wood of *Pinus radiata* D. Don, the cell wall layering structure is similar to that of fiber

in hardwood, while the structure of tracheid cell walls in compression wood is quite different [19]. TEM observations revealed a highly lignified outer S2 layer (S2L) and the absence of an S3 layer in compression wood of *Pinus radiata* D. Don (Fig. 3) [20].
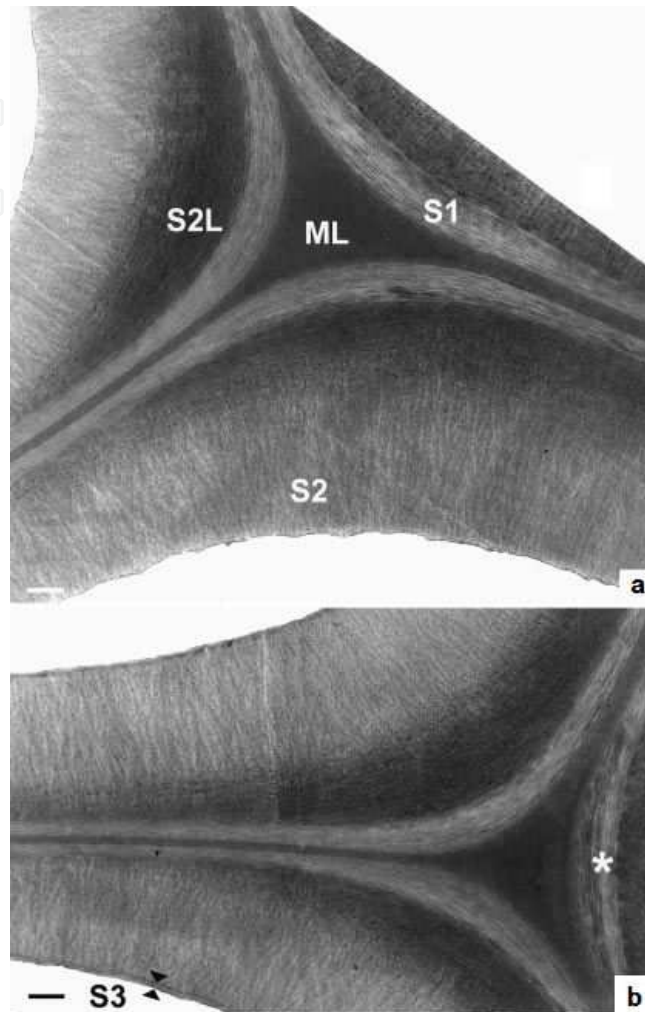

Figure 3. TEM micrographs of mild compression wood of *Pinus radiata* D. Don., taken at 80 kV. ML, middle lamella between adjoining tracheids; S1, outer secondary wall; S2, middle layer of secondary wall; S2L, outer S2 layer.

2.2. Cell wall layering structure in gramineous species

The investigation of the *Miscanthus sinensis* by TEM readily differentiated the sclerenchymatic fiber (Sf) into the middle lamella, the primary wall, and the secondary wall, a typical layering structure of fiber cell walls in wood and grass species (Fig. 4a) [13, 21, 22]. Interestingly, there was a greater degree of heterogeneity in the layering structure of Sf secondary wall (Fig. 4a and 4b), as represented by the fact that we were able to identify six main types (Type I-VI) depending on the number of alternating narrow and broad layers present. Narrow layers appeared as dark thin lines and had a more or less constant thickness. In order to establish the degree of variation in secondary wall patterning among

fiber, a classification system of frequently observed patterns was devised based on TEM observations in Sf adjacent to xylem and phloem (Fig. 5). For the outer Sf connected to the surrounding parenchymatic tissue, the distribution of types I to III (4–6 layers) were predominant, whereas Type IV-VI (7-9 layers) were discernible in individual Sf close to the xylem vessel and phloem cells. Much variation in cell wall layering structure has also been reported for other bamboo species, such as *Phyllostachys viridiglaucescens* and *Dendrocalamus asper*, in which the fibers are categorized into four and six major types according to their respective layering structure [21, 23]. Unlike the layering pattern of Sf adjacent to the xylem vessel in *Miscanthus sinensis*, *Dendrocalamus asper* fibers, which have the highest number of wall layers, were located at the periphery of the fiber bundles. Moreover, the poly-lamellated secondary wall is not an exclusive feature of herbaceous species and appears to have evolved in a variety of taxa. The sclerotic bark fibers of beech (*Fagus sylvatica*) have thick cell walls with numerous individual layers irregularly arranged [24]. Tension wood of *Laetia procera* (Poepp.) Eichl. (Flacourtiaceae) also shows a peculiar structure of secondary wall, which alters from thick to thin layers [25]. In the biomass conversion, the complex poly-lamellated structure acts like a barrier limiting the radial penetration of the chemicals and enzyme, which can be referred as the natural biomass recalcitrance.
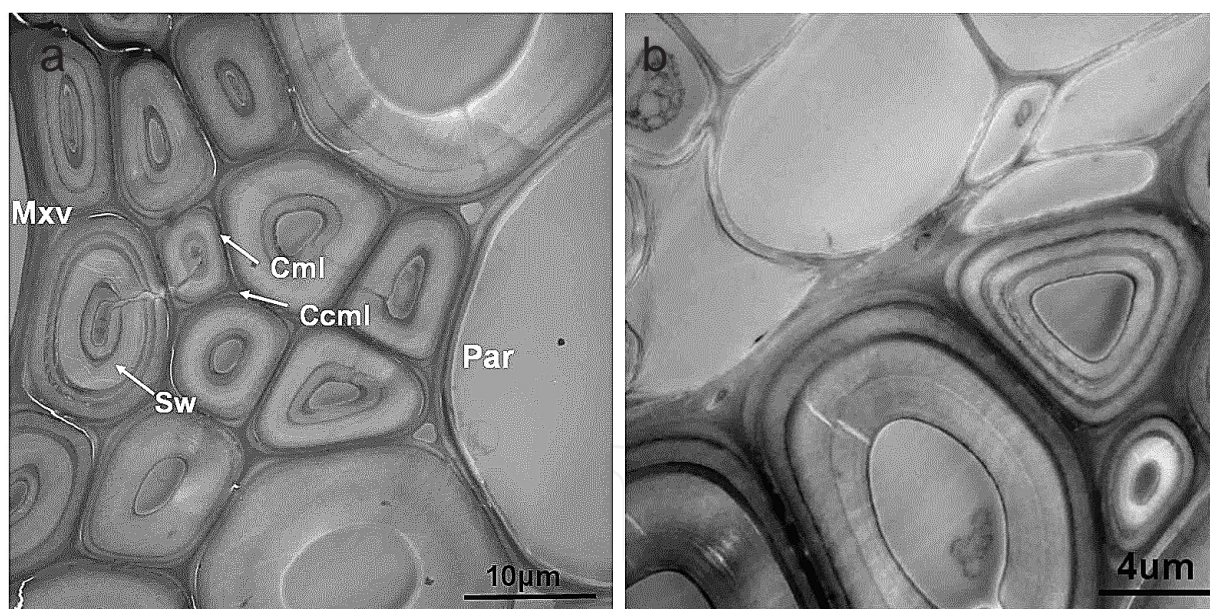

Figure 4. TEM images showing layering structure of Sf in *M. sinensis* cv. internode tissue, stained with 1% w/v KMnO$_4$. (a) Sf adjacent to xylem; (b) Sf adjacent to phloem. Sf, sclerenchymatic fiber; Ccml, cell corner middle lamella; Cml, compound middle lamella; Sw, secondary wall.

In addition to the layering features of Sf secondary wall, the ultrastructural variation in conductive tissue (xylem vessels) was also visualized using TEM images (Fig. 6a and 6b). The secondary wall of Mxv and Pxv could not be clearly divided into sub-layers. This is probably due to either the uniform electron density or the cellulose microfibrils (Mfs) orientation.
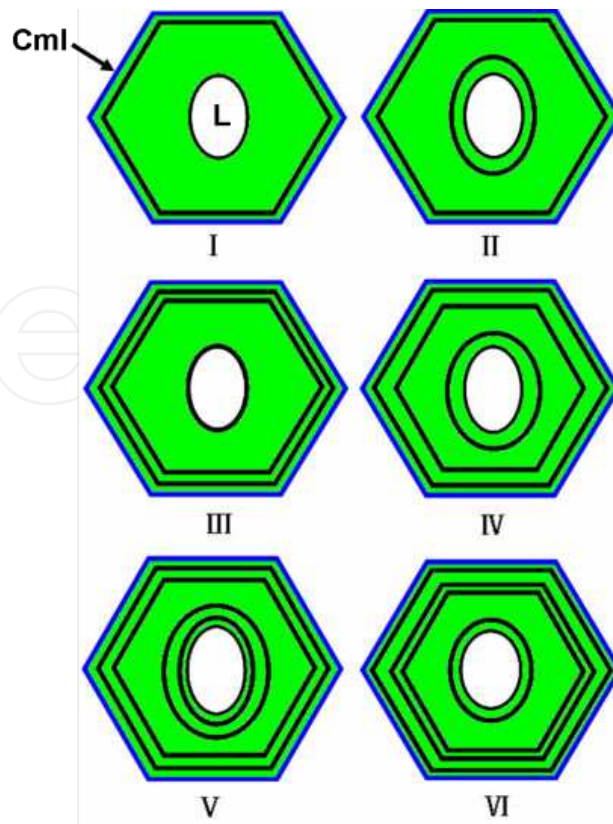
Figure 5. Schematic illustration of Sf layering pattern. "Thin" layers are depicted as black lines, whereas the "broad" layers are colored green. A number has been assigned to the different types of layering for convenience. L: Lumen.
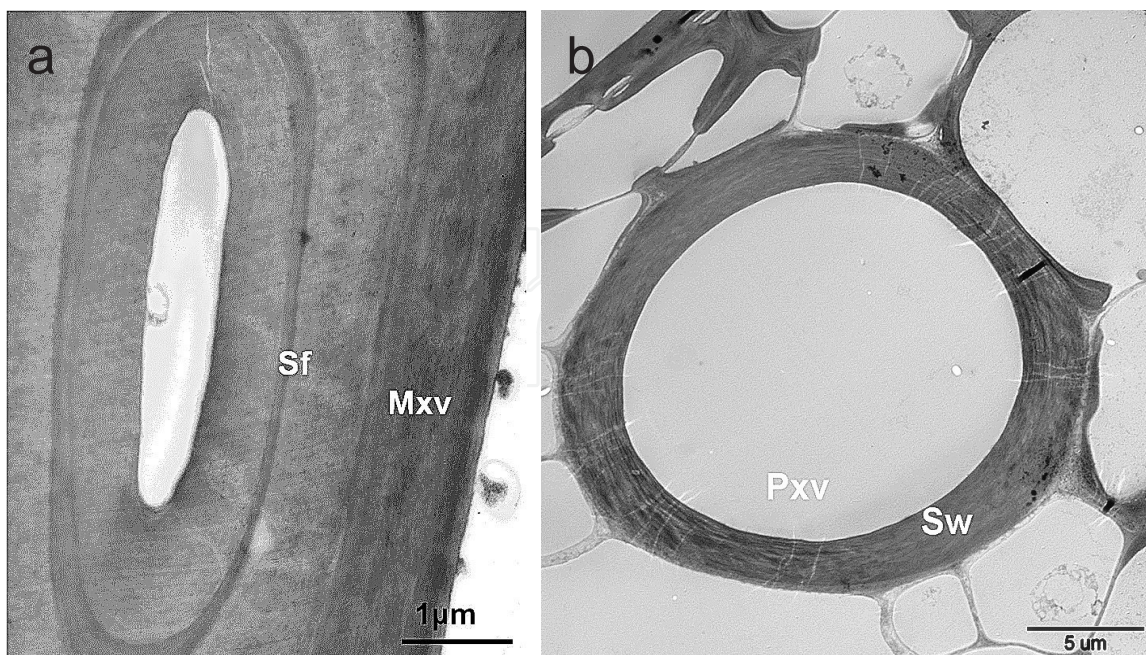

Figure 6. TEM images showing layering structure of *Miscanthus sinensis* internode tissue. (a) Metaxylem vessel (Mxv); (b) protoxylem vessel (Pxv).

3. Lignification and lignin distribution

Next to cellulose, lignin is the most abundant and important polymeric organic substance in plant cell wall. It is a complex phenolic polymer formed by radical coupling reactions of three main monolignols: *p*-coumaryl, coniferyl, and sinapyl alcohol [26, 27]. As a major component of the cell wall of higher plants, lignin plays a vital role in plant growth by enhancing the strength of plant tissues and sealing the wall from water leaks and pathogens invasion. During plant cell wall formation, lignification is generally regarded as the final stage of the differentiating process, where lignin is deposited within the polysaccharide cell wall framework by infilling interlamellar voids [28]. Studies of lignin distribution in plant cell walls are important because of the effect of uneven lignin distribution on wood properties, particularly pulping properties and resistance to decay. Until now, considerable effort has been applied to the investigation of lignin distribution in the cell wall. Since the early 1980s, advanced electron microscopic techniques were developed to obtain high-resolution information on the lignin distribution in plant cell walls. TEM coupled with potassium permanganate ($KMnO_4$) staining has proven to be effective in obtaining high-resolution information on the lignin deposition [13, 19, 29]. On the other hand, the bromination technique by combination of energy-dispersive X-ray analysis (EDXA) with TEM or scanning electron microscopy (SEM) has shown the potential of providing quantitative information on the distribution of lignin. A similar method was developed with the mercurization of specimen and subsequent SEM/TEM-EDXA analyses, which is also based on chemical reactions between lignin and inorganic compounds [16, 30, 31]. Moreover, using newly developed immunological labeling markers to probe lignin with respect to its monomeric composition and with respect to the nature of its structural internal linkages, immunogold TEM has proven to be powerful in distinguishing different lignin substructures on the ultrastructural level [32-35].

3.1. Lignification

The lignification of plant cell walls is generally known to last for a long period, from the S_1 stage to the F stage. After the enlargement of cell size, the secondary wall is thickened with the formation of the S1, S2, and S3 layers. The outermost region of the cell wall, including the intercellular layer, the cell comers, and the primary wall, is lignified during the S1 stage when the surface enlargement of the cell is completed, and just before the S1 starts thickening. This lignification, which will be called "intercellular layer (I)-lignification," may play an important role in stabilizing the cell size and adhering adjacent cells with one another. This I-lignification continues during the differentiation of the S1 and S2 layers, and even until the formation of the S3. On the other hand, the lignification of the secondary wall, which will be called "S-lignification", proceeds mainly after the development of a secondary wall framework, that is, in the final (F) stage of differentiation, although its initiation can be detected already during the S2 stage.

To obtain more detailed information, the immunogold-labeling technique has been applied to differentiate between macromolecular features of condensed (mainly C–C bonds) and non-condensed (*O*-4 aryl–alkyl bonds) lignin subunits during deposition. The results obtained with

a young poplar tree suggest that condensed G and GS types of lignin substructures are preferably formed in middle lamella and cell corners of the differentiating fibers, whereas the formation of non-condensed bonds is favorable in the incipient S1, just at the onset of secondarization [36]. Recently, a polyclonal antibody against a specific condensed lignin substructure, that is, the 8-ring dibenzodioxocin, has been raised for TEM-immunogold detection of the lignification process in cell walls of softwood xylem [33, 34, 37]. The results demonstrated the absence of the dibenzodioxocin structure in very young tracheids where secondary cell wall layers were not yet formed. Moreover, the dibenzodioxocin structure was more abundant in the secondary cell wall layers than in the middle lamella during secondary cell wall thickening. In contrast to the concept of late lignification, that is, in which wood tracheid cell walls undergo lignification only after deposition of polysaccharides, this is an indication that lignification possibly occurs parallel to polysaccharide deposition. In addition to direct lignin labeling, key enzymes involved in the lignification of plant cell walls were localized in developing walls with specific antibodies. In developing xylem cells of Populus, strong labeling of peroxidases in cell corner regions during early developing stages is probably confirming the onset of lignification in these wall portions [38].

3.2. Lignin distribution

3.2.1. Distribution of lignin in softwoods

A number of topochemical detections established that the compound middle lamella is more highly lignified than the secondary wall in typical softwood tracheids [15, 17, 19, 20, 39]. Moreover, the SEM-EDXA technique provided quantitative information of lignin distribution with relatively high accuracy. The distribution of lignin in loblolly pine (*Pinus taeda* L.) tracheids was determined by bromination coupled with SEM-EDXA. It is interesting to note that the lignin concentration in the S2 layer is lower than that in either the S1 or S3 layer [40]. Similar finding was also reported for tracheids of Japanese fir (*Abies suchalinensis* Fr. Schm.) [41].

3.2.2. Distribution of lignin in hardwoods

In contrast to the tracheid as the main cell in softwoods, hardwoods have a variety of cells, such as vessels, parenchyma, and fibers. The lignin distribution between secondary wall and middle lamella in hardwood fibers is similar to that in softwoods; however the secondary wall of hardwood fibers is often less lignified than the secondary wall of softwood tracheids. Figure 7 shows the distribution of lignin in *populous nigra* stem as determined by TEM with potassium permanganate staining [5]. The TEM image exhibits the inhomogeneous distribution of lignin.

3.2.3. Distribution of lignin in reaction woods

Reaction woods appear on leaning stems or branches by any force such as a landslide or snowfall. In softwoods, the reaction wood forms at the lower side of leaning stems or branches, where the compression stress reacts on the xylem. Therefore, this reaction wood is generally called compression wood. Compression wood differs from normal wood in its anatomical
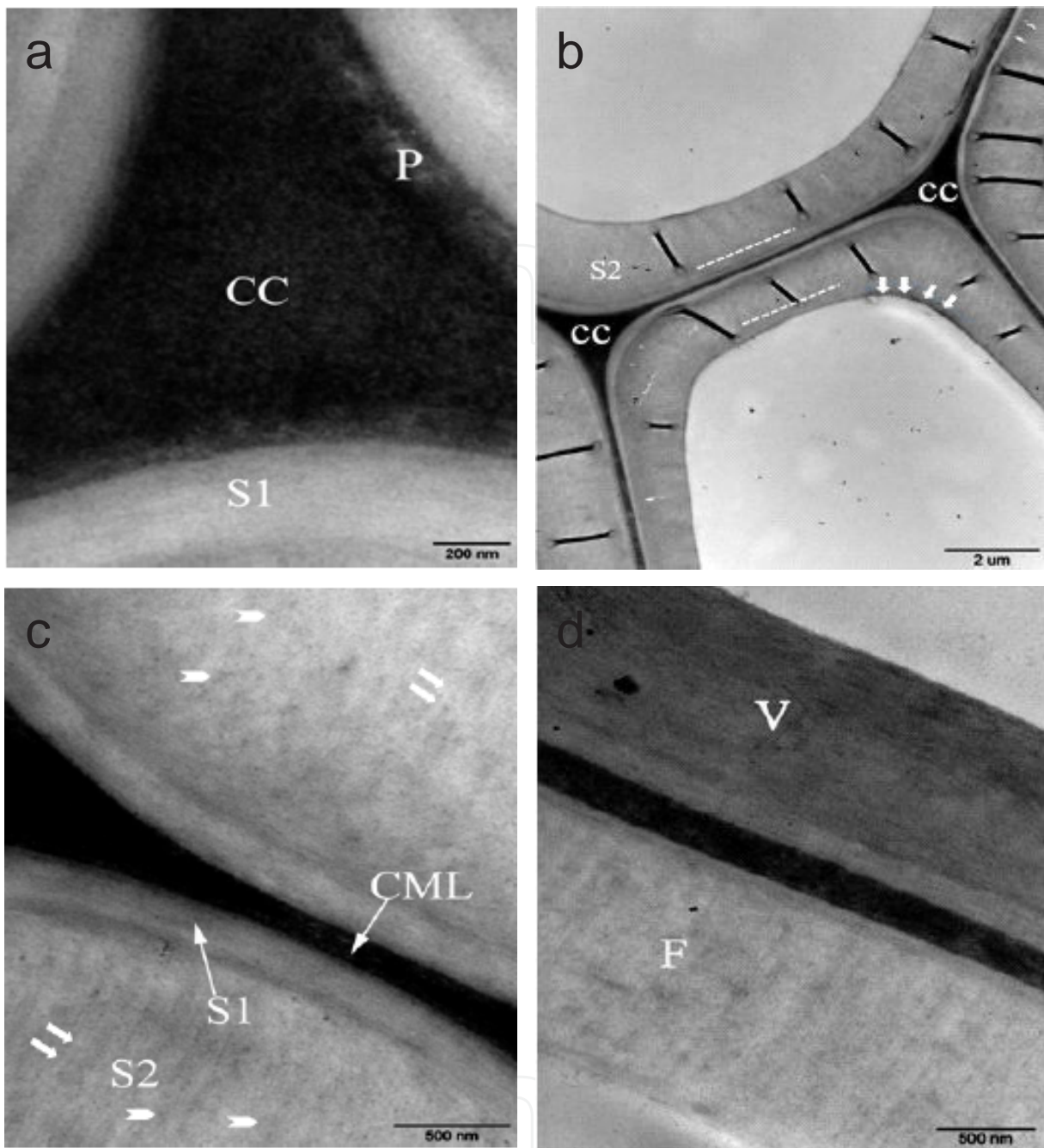
Figure 7. TEM images showing the inhomogeneous distribution of lignin, taken at 80 kV. (a) The CC and P showed higher electron density than the adjacent S1. (b) The outer and inner parts of the S2 layer appear more electron dense (stipplings) than the mid part, the density being particularly pronounced in the curved region of the wall (arrows). (c) The lignin distribution in the S2 layer is distinctly inhomogeneous, with the wall appearing to be a mosaic of electron-dense (arrowheads) and electron-lucent (arrows) regions. The lucent regions have a pattern of sinuous features along the radial directions. (d) The dark staining of the vessel indicated that it is highly lignified, V: vessel, F: fiber.

appearance. Differences include a more lignified secondary cell wall (S2L) layer, absence of an S3 layer, and the presence of intercellular spaces in the cell corner region [42, 43]. The distribution of lignin in compression wood has been extensively investigated. Compression wood shows marked changes in the distribution of lignin across the cell wall with reduced lignifi-

cation of the middle lamella and increased lignification of the S2L layer. In mild compression wood, the lignification of the CCML and the S2L regions is generally comparable, while the S1 and S2 layers were less lignified (Fig. 3) [20]. In severe compression wood, intercellular spaces reduce the contribution of middle lamella lignin to overall lignin content, which is nevertheless increased by the greater lignification of the S2L layer.

On the contrary, reaction wood named as tension wood is formed at the upper side of leaning stems or branches in hardwoods where the xylem loads the tensile stress. Tension wood is characterized by the presence of a cellulose abundant gelatinous layer (GL) forming part of the secondary wall in fibers [44-46]. In maple and oak TW fibers, the GL was divided into concentric sub-layers that appeared either as single rings or as several concentric zones of high and low contrast. Weak staining with potassium permanganate was also visualized at the interface of adjoining concentric layers in maple but was more widespread across the GL in oak, indicating the deposition of aromatic compounds within the cellulose structure of the GL [47].

4. Hemicelluloses deposition

Hemicelluloses are a heterogeneous group of polysaccharides, including xyloglucans, xylans, mannans, and glucomannans. They form physical and chemical bonds to cellulose and lignin and therefore have an important role in building the three-dimensional structures of plant cell walls [48]. The detailed structure of the hemicelluloses and their abundance vary widely among species and cell types. Combination of TEM and immunolabeling has provided detailed information about the deposition of main hemicelluloses related to tissue development and differentiation.

4.1. Hemicelluloses deposition in softwoods

Glucomannans (GMs) are the most abundant hemicelluloses found in softwoods. GMs are composed of a linear backbone of randomly β-(1,4)-linked D-glucosyl and D-mannosyl residues. The ratio of glucosyl and mannosyl units in softwood GMs is approximately 1:3, and D-galactosyl residues are occasionally attached to the backbone with α-(1,6)-glycosidic bonds. In addition to the galactosyl side chain of GMs, softwood GMs also contain partially substituted hydroxyl groups with O-acetyl groups at C-2 and C-3 of the mannosyl residues [49].

Many studies have reported the distribution of GMs in the softwood cell wall using various immunochemical probes specific to GMs in combination with TEM. Using the enzyme-gold complex method, Joseleau and Ruel (1984) have demonstrated that GMs of spruce (*Picea abies*) are present mainly in secondary walls but not in the compound middle lamella [50]. The distribution of GMs in the differentiating tracheid cell wall of *Chamaecyparis obtuse* was also investigated by immunogold labeling [51]. The electron microscopic observation showed that labeling of GMs was restricted to the secondary walls of the tracheids and the labeling density temporarily increased and then decreased in the outer and middle layers of the secondary wall during cell wall formation. Investigation of Lodgepole pine (*Pinus contorta var. latifolia*

Englem.) differentiating secondary xylem showed GM deposition not only in the secondary cell wall, but also in the Golgi apparatus, including vesicles [52]. Recently, the detailed spatial and temporal distribution of GMs in differentiating tracheid cell walls of *Cryptomeria japonica* was investigated using immunogold labeling in conjunction with TEM, and the influence of acetylation on immunolocalization of GMs was reported (Fig. 8) [53]. At the primary cell-wall formation stage in tracheids, GM labeling was absent in the cell wall. GMs began to deposit at the corner of the cell wall in the early S1 formation stage. Compared to the stronger GM labeling present in the innermost and outermost parts of the S1 layer, the middle of the S1 layer showed only minimal labeling, and then increased gradually during S1 formation. Thus, the authors speculate that some softwood GMs may show an intussusceptional deposition mode by penetrating into the intermicrofibrillar spaces during cell wall formation without binding to microfibrils. A clear uneven distribution of GMs in the S2 layer during S2 formation was also observed. GM labeling increased gradually in the S2 layer during S2 formation with the innermost part of the S2 layer showing the highest density of GM labeling. The deposition of GMs in S3 layer also showed a similar trend with weak labeling at the early stage of S3 formation, and then increased labeling during maturation. The increased GM labeling during cell wall maturation is not consistent with the previous study of the differentiating tracheid cell wall of *Chamaecyparis obtuse* suggesting that the density of GM labeling decreased gradually during cell wall formation because of lignin deposition during cell wall maturation. GM labeling in mature tracheids of *Cryptomeria japonica* showed higher concentration of GMs in the S1 layer than that in the S2 layer, which is in agreement with immunogold labeling study of *Chamaecyparis obtusa*. In addition, GM labeling was also observed in the CML of *Cryptomeria japonica* mature tracheids whereas GMs showing absence in the CML in either developing or mature tracheid cell walls of *Chamaecyparis obtuse* [51, 53]. To explore the influence of acetylation on immunolocalization of GMs, specimens treated with mild alkali solution were also investigated. Deacetylation of GMs with mild alkali treatment led to a significant increase in GM labeling, suggesting that some GM epitopes may be masked by acetylation. It is interesting to note that the changes in GM labeling after deacetylation were not very pronounced until the early stages of S2 formation, indicating that GMs deposited in the cell wall at early stages of cell wall formation may contain fewer acetyl groups than those deposited at later stages. Furthermore, the decreased GM labeling in mature tracheids suggests that some acetyl groups may be removed from GMs after cell wall formation [53].

In addition to GMs, the distribution of xylans in tracheid walls was also investigated. Xylans in wood cell walls are basically composed of a backbone of xylose units that are linked by β-(1-4)-glycosidic bonds. Softwood xylans that are called arabino-4-*O*-methylglucuronoxylans (AGXs) contain arabinofuranose units linked by α-(1-3)-glycosidic bonds to the xylan backbone [49]. The distribution of AGXs in differentiating earlywood tracheid cell walls of *Cryptomeria japonica* was systematically investigated using immune-TEM [54]. Xylans were found to first deposit in the corner of the S1 layer in the early stages of S1 formation in tracheids. In addition, large amount of xylans were also observed in CCML from the early stage of cell wall formation. During S1 formation, the innermost S1 layer showed weaker xylan labeling than did the rest of the cell wall. A similar pattern was observed during secondary cell wall formation, with the innermost layer and the boundary between the S1 and S2 layers showing
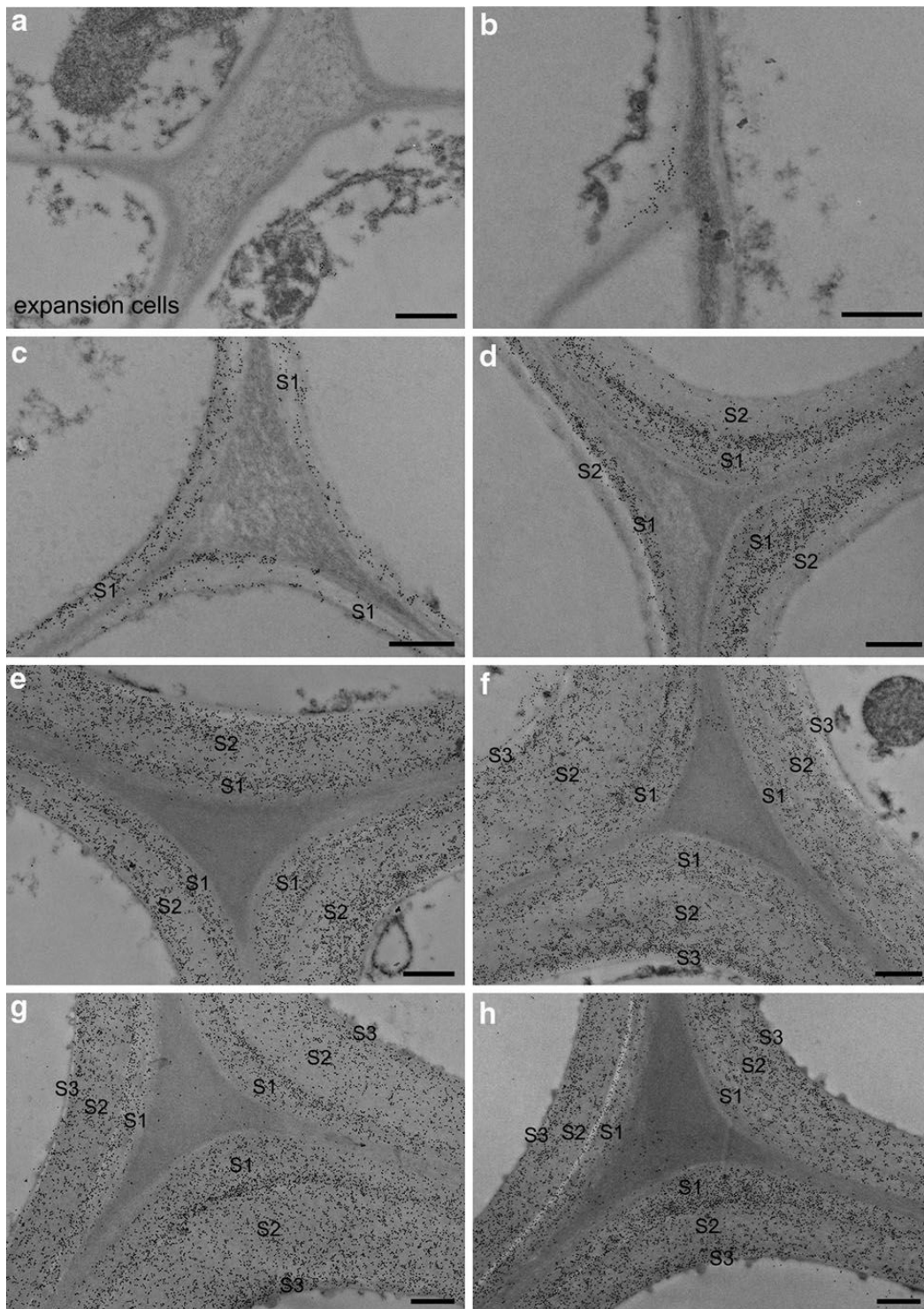
Figure 8. Immunogold localization of glucomannans (GMs) in differentiating and differentiated tracheids. (a) Expansion cells. (b) Tracheids at the early S1 formation stage. (c) Tracheids at the S1 layer formation stage. (d) Tracheids at the early S2 formation stage. (e) Tracheids at the formation of the S2 layer. (f) Tracheids at the formation of the S3 layer. (g, h) Mature tracheids.

weaker labeling than other parts of the cell wall. These results indicate the spatial consistency between xylan deposition and lignin deposition in the early stages of tracheid cell wall

formation [55]. However, an almost uniform distribution of xylans throughout the entire cell wall was observed in mature tracheids.

Furthermore, to extend the understanding of distributional diversities of hemicelluloses among cells, the deposition of GMs and AGXs in ray cells and pits was investigated by immunolabeling [56]. In comparison with tracheids, ray cells have different deposition processes of GMs and AGXs. GM labeling in ray cells began to be detected at the early stage of S1 formation in tracheids, whereas AGX labeling began to be detected in ray cells at the S2 formation stage in tracheids. In mature ray cells, GM labeling was absent in the innermost layer of ray cells, whereas AGXs were uniformly distributed in the entire ray cell walls. In pits, GM labeling was detected in pit membranes at an early stage of pit formation, but disappeared during pit maturation, indicating that enzymes capable of GM degradation may be involved in pit formation. In contrast to GM labeling, AGX labeling was not observed in pit membranes during the entire pit developmental process.

4.2. Hemicelluloses deposition in hardwoods

In hardwoods, *O*-acetyl-4-*O*-methylglucuronoxylans (AcGXs) are the main hemicellulose, occupying about 30% of total cell wall components. AcGXs consist of a β-(1,4)-xylan backbone, decorated with acetyl groups and side chains of 4-*O*-methyl-α-D glucuronic acid [49]. The localization of xylans has been studied by various in situ labeling methods, for example, the xylanase-gold method [57, 58], xylanase and anti-xylanase antibodies [59], and the immuno-gold method [60-62]. In differentiating xylem of Japanese beech, xylan deposition started in the middle of the S1 layer formation stage and labeling of GXs was seen only in the secondary walls of xylem cells, but not in the primary walls or the middle lamella. In addition, the increased labeling density during cell wall formation strongly suggested that the deposition of GXs may occur in a penetrative way [60]. The distribution of xylans in differentiating *Populus* xylem cells has been systematically investigated using immuno-microscopic methods in combination with monoclonal antibodies (LM10 and LM11) specific to β-(1-4)-linked xylopyr-anosyl residues [62]. LM10 antibody binds low-substituted xylans (lsAcGXs), whereas LM11 antibody binds high-substituted xylans (hsAcGXs) in addition to lsAcGXs [63]. Xylan depo-sition was detected earliest in fibers at the cell corner of the S1 layer, and then later in vessels and ray cells, respectively. During secondary cell wall development of fibers, xylan deposition began from the cell corner of the S1 layer after initiation of S1 formation and different labeling patterns of LM10 and LM11 antibodies were observed. LM10 showed stronger xylan locali-zation in the outer secondary cell wall than inner layer, while LM11 showed uniform xylan labeling in the whole secondary cell wall. Differentiating vessels showed similar patterns of xylan labeling as fibers except that vessels showed more uniform labeling in the mature cell wall with stronger labeling of lsAcGXs than fibers. In ray cells, xylan labeling occurred at the S2 formation stage in fibers, which was much later than that in fibers and vessels, but was also detected at the beginning of secondary cell wall formation in ray cells. Unlike fibers and vessels, ray cells showed a more homogeneous composition and distribution of xylans than fibers and vessels. All of the three pit types in the secondary xylem of aspen (including fiber–fiber, vessel–vessel, and ray–vessel) showed strong labeling of hsAcGXs during differentiation, and yet gradually disappeared during pit maturation.

4.3. Hemicelluloses deposition in gramineous species

Most of the existing research about distribution of hemicelluloses in gramineous species concentrate on Arabidopsis, which is one of the most frequently used model plants in plant science. Several immunocytochemical studies have reported the distribution of xylans in Arabidopsis stem [64-66]. Xylan deposition in xylary fibers (fibers) was initiated at the cell corner of the S1 layer and the xylan labeling increased gradually during fiber maturation. Metaxylem vessels showed more developed stages of secondary cell wall formation than fibers, but revealed almost identical xylan labeling patterns to fibers during maturation. The consistency of the immunolabeling patterns between LM10 and LM11 in the cell wall of fibers, vessels, and protoxylem vessels indicated that vascular bundle cells may be chemically composed of a highly homogeneous xylan type. In contrast, interfascicular fibers showed different labeling patterns between the two antibodies and also between different developmental stages. Immunolocalization studies of mannans in Arabidopsis stems have shown that mannans are distributed in the various cell types with different concentrations [67-69]. Temporal and spatial variations in mannan labeling between cell types in the secondary xylem of Arabidopsis stems were examined using immunolocalization with mannan-specific monoclonal antibodies (LM21 and LM22). Mannan labeling in secondary xylem cells (except for protoxylem vessels) was initially detected in the cell wall during S2 formation and increased gradually during development. Labeling in metaxylem vessels (vessels) was detected earlier than that in xylary fibers (fibers), but was much weaker than fibers. The S1 layer of vessels and fibers showed much less labeling than the S2 layer. Some strong labeling was also detected in pit membranes of vessel pits.

5. Conclusions

The potential of TEM for investigation of plant cell walls has already been demonstrated on various plant tissues. The high spatial resolution allows detection of changes in the ultrastructure and cell wall polymer deposition on the cell and cell wall level. Nevertheless, complex sample preparation procedure will limit its extensive application, especially in living plant tissues. Thus, when combined with other in situ microscopic techniques (such as atom force microscopy, confocal laser microscopy, confocal Raman microscopy), much more information hidden in plant cell wall will be illustrated.

Author details

Xia Zhou, Dayong Ding, Jing Ma, Zhe Ji, Xun Zhang and Feng Xu[*]

*Address all correspondence to: xfx315@bjfu.edu.cn

Beijing Key Laboratory of Lignocellulosic Chemistry/MOE Key Laboratory of Wooden Material Science and Application, Beijing Forestry University, Beijing, China

References

[1] Rüggeberg M, Saxe F, Metzger TH, Sundberg B, Fratzl P, Burgert I. Enhanced cellulose orientation analysis in complex model plant tissues. Journal of Structural Biology 2013;183(3) 419-428.

[2] Mayo SC, Chen F, Evans R. Micron-scale 3D imaging of wood and plant microstructure using high-resolution X-ray phase-contrast microtomography. Journal of Structural Biology 2010;171(2) 182-188.

[3] Himmel ME, Ding SY, Johnson DK, Adney WS, Nimlos MR, Brady JW, Foust TD. Biomass recalcitrance: Engineering plants and enzymes for biofuels production. Science 2007;315(5813) 804-807.

[4] Cosgrove DJ. Growth of the plant cell wall. Nature Reviews Molecular Cell Biology 2005;6(11) 850-861.

[5] Ma J, Zhang Z, Yang G, Mao J, Xu F. Ultrastructural topochemistry of cell wall polymers in *Populus nigra* by transmission electron microscopy and Raman imaging. BioResources 2011;6(4) 3944-3959.

[6] Fangel JU, Ulvskov P, Knox JP, Mikkelsen MD, Harholt J, Popper ZA, Willats WG. Cell wall evolution and diversity. Frontiers in Plant Science 2012;3 152.

[7] Kim JS, Lee KH, Cho CH, Koch G, Kim YS. Micromorphological characteristics and lignin distribution in bamboo (*Phyllostachys pubescens*) degraded by the white rot fungus *Lentinus edodes*. Holzforschung 2008;62(4) 481.

[8] Yu H, Liu R, Shen D, Wu Z, Huang Y. Arrangement of cellulose microfibrils in the wheat straw cell wall. Carbohydrate Polymers 2008;72(1) 122-127.

[9] Hanley SJ, Giasson J, Revol J-F, Gray DG. Atomic force microscopy of cellulose microfibrils: comparison with transmission electron microscopy. Polymer 1992;33(21) 4639-4642.

[10] Gierlinger N, Schwanninger M. The potential of Raman microscopy and Raman imaging in plant research. Spectroscopy: An International Journal 2007; 21(2): 69-89.

[11] Agarwal UP, Atalla RH. In-situ Raman microprobe studies of plant cell walls: Macromolecular organization and compositional variability in the secondary wall of *Picea mariana* (Mill.) B.S.P. Planta 1986;169(3) 325-332.

[12] Singh AP, Donaldson LA. Ultrastructure of tracheid cell walls in radiata pine (*Pinus radiata*) mild compression wood. Canadian Journal of Botany 1999;77(1) 32-40.

[13] Singh A, Daniel G, Nilsson T. Ultrastructure of the S2 layer in relation to lignin distribution in *Pinus radiata* tracheids. Journal of Wood Science 2002;48(2) 95-98.

[14] Brandt B, Zollfrank C, Franke O, Fromm J, Göken M, Durst K. Micromechanics and ultrastructure of pyrolysed softwood cell walls. Acta Biomaterialia 2010;6(11) 4345-4351.

[15] Fromm J, Rockel B, Lautner S, Windeisen E, Wanner G. Lignin distribution in wood cell walls determined by TEM and backscattered SEM techniques. Journal of Structural Biology 2003;143(1) 77-84.

[16] Eriksson I, Lidbrandt O, Westermark U. Lignin distribution in birch (*Betula verrucosa*) as determined by mercurization with SEM- and TEM-EDXA. Wood Science and Technology 1988;22(3) 251-257.

[17] Tirumalai VC, Agarwal UP, Obst JR. Heterogeneity of lignin concentration in cell corner middle lamella of white birch and black spruce. Wood Science and Technology 1996;30(2) 99-104.

[18] Donaldson L, Hague J, Snell R. Lignin distribution in coppice poplar, linseed and wheat straw. Holzforschung 2001;55(4).

[19] Donaldson LA, Singh AP, Yoshinaga A, Takabe K. Lignin distribution in mild compression wood of *Pinus radiata*. Canadian Journal of Botany-Revue Canadienne De Botanique 1999;77(1) 41-50.

[20] Singh AP, Donaldson LA. Ultrastructure of tracheid cell walls in radiate pine (*Pinus radiata*) mild compression wood. Canadian Journal of Botany-Revue Canadienne De Botanique 1999;77(1) 32-40.

[21] Murphy RJ, Alvin KL. Variation in fibre wall structure in bamboo. IAWA Journal 1992;13(4) 403-410.

[22] Gritsch CS, Murphy RJ. Ultrastructure of fibre and parenchyma cell walls during early stages of culm development in *Dendrocalamus asper*. Annals of Botany 2005;95(4) 619-629.

[23] Gritsch CS, Kleist G, Murphy RJ. Developmental changes in cell wall structure of phloem fibres of the bamboo *Dendrocalamus asper*. Annals of Botany 2004;94(4) 497-505.

[24] Prislan P, Koch G, Schmitt U, Gričar J, Čufar K. Cellular and topochemical characteristics of secondary changes in bark tissues of beech (*Fagus sylvatica*). Holzforschung 2012;66(1) 131.

[25] Ruelle J, Yoshida M, Clair B, Thibaut B. Peculiar tension wood structure in *Laetia procera* (Poepp.) Eichl. (Flacourtiaceae). Trees 2007;21(3) 345-355.

[26] Nimz HH, Robert D, Faix O, Nemr M. Carbon-13 NMR spectra of lignins, 8. Structural differences between lignins of hardwoods, softwoods, grasses and compression wood. Holzforschung-International Journal of the Biology, Chemistry, Physics and Technology of Wood 1981;35(1) 16.

[27] Boerjan W, Ralph J, Baucher M. Lignin biosynthesis. Annual Review of Plant Biology 2003;54(1) 519-546.

[28] Donaldson LA. Lignification and lignin topochemistry-an ultrastructural view. Phytochemistry 2001;57(6) 859-873.

[29] Lee KH, Singh AP, Kim YS. Cellular characteristics of a traumatic frost ring in the secondary xylem of *Pinus radiata*. Trees 2007;21(4) 403-410.

[30] Saka S, Thomas RJ. Evaluation of the quantitative assay of lignin distribution by SEM-EDXA-technique. Wood Science and Technology 1982;16(1) 1-18.

[31] Donaldson LA, Ryan KG. A comparison of relative lignin concentration as determined by interference microscopy and bromination/EDXA. Wood Science and Technology 1987;21(4) 303-309.

[32] Kapat A, Dey S. An alternative approach to the detection of lignin: a note on the application of ELISA using polyclonal antibodies. Bioprocess Engineering 2000;22(1) 75-77.

[33] Kukkola E, Koutaniemi S, Gustafsson M, Karhunen P, Ruel K, Lundell T, Saranpää P, Brunow G, Teeri T, Fagerstedt K. Localization of dibenzodioxocin substructures in lignifying Norway spruce xylem by transmission electron microscopy-immunogold labeling. Planta 2003;217(2) 229-237.

[34] Kukkola E, Koutaniemi S, Pöllänen E, Gustafsson M, Karhunen P, Lundell T, Saranpää P, Kilpeläinen I, Teeri T, Fagerstedt K. The dibenzodioxocin lignin substructure is abundant in the inner part of the secondary wall in Norway spruce and silver birch xylem. Planta 2004;218(3) 497-500.

[35] Ligrone R, Carafa A, Duckett JG, Renzaglia KS, Ruel K. Immunocytochemical detection of lignin-related epitopes in cell walls in bryophytes and the charalean alga *Nitella*. Plant Systematics and Evolution 2008;270(3-4) 257-272.

[36] Ruel K, Montiel MD, Goujon T, Jouanin L, Burlat V, Joseleau JP. Interrelation between lignin deposition and polysaccharide matrices during the assembly of plant cell walls. Plant Biology 2002;4(1) 2-8.

[37] Kukkola E, Saranpää P, Fagerstedt K. Juvenile and compression wood cell wall layers differ in lignin structure in norway spruce and scots pine. IAWA Journal 2008;29(1) 47-57.

[38] Kim YS, Wi SG, Grünwald C, Schmitt U. Immuno electron microscopic localization of peroxidases in the differentiating xylem of populus spp. Holzforschung 2002;56(4) 355.

[39] Donaldson LA. Mechanical constraints on lignin deposition during lignification. Wood Science and Technology 1994;28(2) 111-118.

[40] Saka S, Thomas RJ. A study of lignification in loblolly pine tracheids by the SEM-ED-XA technique. Wood Science and Technology 1982;16(3) 167-179.

[41] Fukazawa K, Imagawa H. Quantitative analysis of lignin using an UV microscopic image analyser. Variation within one growth increment. Wood Science and Technology 1981;15(1) 45-55.

[42] Timell TE. Recent progress in the chemistry and topochemistry of compression wood. Wood Science and Technology 1982;16(2) 83-122.

[43] Donaldson LA., Singh AP. Formation and structure of compression wood. In: Fromm J. (ed.), Cellular aspects of wood formation. Berlin Heidelberg: Springer; 2013. p225-256.

[44] Bowling AJ, Vaughn KC. Immunocytochemical characterization of tension wood: Gelatinous fibers contain more than just cellulose. American Journal of Botany 2008;95(6) 655-663.

[45] Mellerowicz EJ, Gorshkova TA. Tensional stress generation in gelatinous fibres: A review and possible mechanism based on cell-wall structure and composition. Journal of Experimental Botany 2012;63(2) 551-565.

[46] Yoshinaga A, Kusumoto H, Laurans F, Pilate G, Takabe K. Lignification in poplar tension wood lignified cell wall layers. Tree Physiology 2012;32(9) 1129-1136.

[47] Lehringer C, Daniel G, Schmitt U. TEM/FE-SEM studies on tension wood fibres of *Acer spp.*, *Fagus sylvatica* L. and *Quercus robur* L. Wood Science and Technology 2009;43(7-8) 691-702.

[48] Pauly M, Gille S, Liu L, Mansoori N, De Souza A, Schultink A, Xiong G. Hemicellulose biosynthesis. Planta 2013;238(4) 627-642.

[49] Fengel D, Wegener G. Wood: chemistry, ultrastructure, reactions. Berlin: De Gruyter; 1984.

[50] Ruel K, Joseleau JP. Use of enzyme-gold complexes for the ultrastructural localization of hemicelluloses in the plant cell wall. Histochemistry 1984;81(6) 573-580.

[51] Maeda Y, Awano T, Takabe K, Fujita M. Immunolocalization of glucomannans in the cell wall of differentiating tracheids in *Chamaecyparis obtusa*. Protoplasma 2000;213(3-4) 148-156.

[52] Samuels A, Rensing K, Douglas C, Mansfield S, Dharmawardhana D, Ellis B. Cellular machinery of wood production: differentiation of secondary xylem in *Pinus contorta var. latifolia*. Planta 2002;216(1) 72-82.

[53] Kim JS, Awano T, Yoshinaga A, Takabe K. Temporal and spatial immunolocalization of glucomannans in differentiating earlywood tracheid cell walls of *Cryptomeria japonica*. Planta 2010;232(2) 545-554.

[54] Kim JS, Awano T, Yoshinaga A, Takabe K. Immunolocalization and structural varia‐
tions of xylan in differentiating earlywood tracheid cell walls of *Cryptomeria japonica*.
Planta 2010;232(4) 817-824.

[55] Donaldson LA. Lignification and lignin topochemistry-an ultrastructural view. Phy‐
tochemistry 2001;57(6) 859-873.

[56] Kim JS, Awano T, Yoshinaga A, Takabe K. Temporal and spatial diversities of the im‐
munolabeling of mannan and xylan polysaccharides in differentiating earlywood ray
cells and pits of *Cryptomeria japonica*. Planta 2011;233(1) 109-122.

[57] Vian B, Reis D, Mosiniak M, Roland JC. The glucuronoxylans and the helicoidal shift
in cellulose microfibrils in linden wood: *Cytochemistryin muro* and on isolated mole‐
cules. Protoplasma 1986;131(2) 185-199.

[58] Vian B, Roland J-C, Reis D, Mosiniak M. Distribution and possible morphogenetic
role of the xylans within the secondary vessel wall of linden wood. IAWA Journal
1992;13(3) 269-282.

[59] Taylor JG, Haigler CH. Patterned secondary cell-wall assembly in tracheary elements
occurs in a self-perpetuating cascade. Acta Botanica Neerlandica 1993;42(2) 153-163.

[60] Awano T, Takabe K, Fujita M. Localization of glucuronoxylans in Japanese beech vi‐
sualized by immunogold labelling. Protoplasma 1998;202(3-4) 213-222.

[61] Awano T, Takabe K, Fujita M, Daniel G. Deposition of glucuronoxylans on the secon‐
dary cell wall of Japanese beech as observed by immuno-scanning electron microsco‐
py. Protoplasma 2000;212(1-2) 72-79.

[62] Kim JS, Sandquist D, Sundberg B, Daniel G. Spatial and temporal variability of xylan
distribution in differentiating secondary xylem of hybrid aspen. Planta 2012;235(6)
1315-1330.

[63] McCartney L, Marcus SE, Knox JP. Monoclonal antibodies to plant cell wall xylans
and Arabinoxylans. Journal of Histochemistry & Cytochemistry 2005;53(4) 543-546.

[64] Brown DM, Zhang Z, Stephens E, Dupree P, Turner SR. Characterization of IRX10
and IRX10-like reveals an essential role in glucuronoxylan biosynthesis in Arabidop‐
sis. The Plant Journal 2009;57(4) 732-746.

[65] Lee C, Teng Q, Huang W, Zhong R, Ye Z-H. The F8H glycosyltransferase is a func‐
tional paralog of FRA8 involved in glucuronoxylan biosynthesis in Arabidopsis.
Plant and Cell Physiology 2009;50(4) 812-827.

[66] Wu A-M, Rihouey C, Seveno M, Hörnblad E, Singh SK, Matsunaga T, Ishii T,
Lerouge P, Marchant A. The Arabidopsis IRX10 and IRX10-LIKE glycosyltransferases
are critical for glucuronoxylan biosynthesis during secondary cell wall formation.
The Plant Journal 2009;57(4) 718-731.

[67] Handford M, Baldwin T, Goubet F, Prime T, Miles J, Yu X, Dupree P. Localisation and characterisation of cell wall mannan polysaccharides in *Arabidopsis thaliana*. Planta 2003;218(1) 27-36.

[68] Goubet F, Barton CJ, Mortimer JC, Yu X, Zhang Z, Miles GP, Richens J, Liepman AH, Seffen K, Dupree P. Cell wall glucomannan in Arabidopsis is synthesised by CSLA glycosyltransferases, and influences the progression of embryogenesis. The Plant Journal 2009;60(3) 527-538.

[69] Marcus SE, Blake AW, Benians TAS, Lee KJD, Poyser C, Donaldson L, Leroux O, Rogowski A, Petersen HL, Boraston A, Gilbert HJ, Willats WGT, Paul Knox J. Restricted access of proteins to mannan polysaccharides in intact plant cell walls. The Plant Journal 2010;64(2) 191-203.